NONLINEAR SEISMIC SOIL-STRUCTURE INTERACTION BY USING A BE-FE METHOD IN THE TIME DOMAIN

Jianjing ZHANG[1], Athol J CARR[2] And Peter J MOSS[3]

SUMMARY

Soil structure interaction is an important topic that has become of increasing interest over the last decade or so. The most favoured research tool has been the Finite Element (FE) method in view of its suitability for solving complex geometric and non-linear problems. However, it does also have a number of disadvantages, one being that finite elements cannot deal with an infinite domain. As a result, many transmitting boundary formulations have been proposed in the last two decades with the Boundary Element (BE) method providing one of the best transmitting boundaries. This paper proposes a coupled BE-FE method to resolve non-linear soil-structure interaction. In this model, boundary elements are used to simulate the infinite domain with finite elements being employed to model the structure and the soil surrounding it

INTRODUCTION

It is known that structural behaviour under an earthquake is affected by the foundation and surrounding soil and the results have been verified by many experiments and site measurements. Many numerical research methods have been proposed to analyse the soil effects on structural responses. Common examples are the lumped-mass method, the substructure method and the finite element method. In these methods, expressions for the far field and the non-linear soil behaviour are very important. Usually, the far field is replaced by a transmitting boundary and the non-linear soil behaviour can be expressed using a hyperbolic model. However, the boundary element method gives a more rigorous expression for the far field and the bounding surface model can represent the non-linear soil behaviour more exactly.

In this paper, the boundary element method will be used to express the far field and a bounding surface model will be used to represent the non-linear soil behaviour. The coupling of the boundary element method and the finite element method utilises a direct coupling that significantly reduces the programming time.

2. COUPLING THE BOUNDARY ELEMENT AND FINITE ELEMENT METHODS

2.1 Boundary Element and Finite Element Formulation

Collocation at each boundary node and at all time steps leads to a system of algebraic equations

$$(\frac{1}{2}[I]+\left[\bar{F}\right])\{u\}=[F]\{u\}=[G]\{t\} \tag{1}$$

[1] Department of Civil Engineering, University of Canterbury, Christchurch
[2] Department of Civil Engineering, University of Canterbury, Christchurch. Email: a.carr@civil.canterbury.ac.nz.
[3] Department of Civil Engineering, University of Canterbury, Christchurch. Email: p.moss@cad.canterbury.ac.nz.

where $\{u\}$ and $\{t\}$ are vectors of the nodal displacements and tractions, respectively. $[G]$ and $[F]$ represent influence matrices which contain integral terms evaluated over each boundary element (numerically) and over each time step (analytically).

Considering the properties of the influence matrices, one obtains from Equation 1 a relationship between $\{u\}$and $\{t\}$ which can be given as:

$$\left[G^1\right]\left\{t^m\right\}+\sum_{p=1}^{m-1}\left[G^{(m-p+1)}\right]\left\{t^{(p)}\right\}=\left[F^1\right]\left\{u^m\right\}+\sum_{p=1}^{m-1}\left[F^{(m-p+1)}\right]\left\{u^{(p)}\right\} \tag{2a}$$

or

$$\left[G^1\right]\left\{t^m\right\}=\left[F^1\right]\left\{u^m\right\}-\sum_{p=1}^{m-1}\left(\left[G^{(m-p+1)}\right]\left\{t^{(p)}\right\}-\left[F^{(m-p+1)}\right]\left\{u^{(p)}\right\}\right) \tag{2b}$$

Furthermore, Equation2b can be expressed as

$$\begin{aligned}\left\{t^m\right\}&=\left[G^1\right]^{-1}\left[F^1\right]\left\{u^m\right\}-\left[G^1\right]^{-1}\left(\sum_{p=1}^{m-1}\left(\left[G^{(m-p+1)}\right]\left\{t^{(p)}\right\}-\left[F^{(m-p+1)}\right]\left\{u^{(p)}\right\}\right)\right)\\&=\left[\vec{K}\right]\left\{u^m\right\}+\left\{\vec{f}\right\}\end{aligned} \tag{3}$$

where

$\left[\vec{K}\right]=\left[G^1\right]^{-1}\left[F^1\right]$ and $\left\{\vec{f}\right\}=\left[G^1\right]^{-1}\left(\sum_{p=1}^{m-1}\left(\left[G^{(m-p+1)}\right]\left\{t^{(p)}\right\}-\left[F^{(m-p+1)}\right]\left\{u^{(p)}\right\}\right)\right)$

According to Equation3, $\left[\vec{K}\right]$ can be considered as the stiffness matrix of a boundary element. $\left\{\vec{f}\right\}$ can be considered as a load that is produced by the time history.

For dynamic analysis using the finite element method, the integration process can be realised either at an element level or, after assembling the local matrices, at a system level. Both methods lead to a so-called effective stiffness matrix [*Keff*] and an effective load vector {*Peff*} while the Newmark β method is used to integrate the equations with respect to time. Thus:

$$\left[K_{eff}\right]\{u\}^m=\left\{P_{eff}\right\}. \tag{4}$$

where

$$\left[K_{eff}\right]=h_4[M]+[K] \qquad \left\{P_{eff}\right\}^m=\{p\}^m-[M]\left(h_6\left\{\ddot{u}\right\}^{m-1}+h_5\left\{\dot{u}\right\}^{m-1}-h_4\{u\}^{m-1}\right)$$

2.2 Coupling Procedure between Boundary Element and Finite Element

The coupling of the boundary element method and the finite element method is performed by imposing compatibility and equilibrium conditions along a contact boundary between the two domains and an assumed weld condition along the contact boundary. Compatibility and equilibrium conditions can be expressed as

$$u_i^{f(m)}=u_i^{b(m)}\ ; \qquad p_i^{f(m)}+p_i^{b(m)}=0 \tag{5}$$

In order to satisfy Equation 5, equilibrium equations, Equation 4 in the finite element domain and Equation 3 in the boundary element domain, will be rearranged to separate the conditions on the contact and non-contact boundaries.

Rewriting Equation 4 for the contact and non-contact boundaries gives:

$$\begin{bmatrix}[K_{00}]^f & [K_{0i}]^f\\ [K_{i0}]^f & [K_{ii}]^f\end{bmatrix}\begin{Bmatrix}\{u_0\}^{f(m)}\\ \{u_i\}^{f(m)}\end{Bmatrix}=\begin{Bmatrix}\{p_0\}^{f(m)}\\ \{p_i\}^{f(m)}\end{Bmatrix}=\begin{Bmatrix}\{p_0\}^{f(m)}\\ \{0\}\end{Bmatrix}+\begin{Bmatrix}\{0\}\\ \{p_i\}^{f(m)}\end{Bmatrix} \tag{6}$$

Therefore, the node load vector at the contact boundary can be expressed as

$$\begin{Bmatrix} \{0\} \\ \{p_i\}^{f(m)} \end{Bmatrix} = \begin{bmatrix} [K_{00}]^f & [K_{0i}]^f \\ [K_{i0}]^f & [K_{ii}]^f \end{bmatrix} \begin{Bmatrix} \{u_0\}^{f(m)} \\ \{u_i\}^{f(m)} \end{Bmatrix} - \begin{Bmatrix} \{p_0\}^{f(m)} \\ \{0\} \end{Bmatrix} \tag{7}$$

However, in rewriting Equation 3, the solution is a traction whereas in Equation 4 the solution is the nodal load. Therefore, the traction has to be converted into a nodal load. For any one element, the relationship between the traction and the nodal load can be expressed as

$$\{p\}^m = [D]\{t\}^m \tag{8}$$

where $[D]$ is a transformation matrix.

At the boundary element domain, the nodal load can be expressed as

$$\left\{p^m\right\} = [D]\left\{t^{b(m)}\right\} = [D]\left[\overrightarrow{K}\right]\left\{u^{b(m)}\right\} - [D]\left\{\overrightarrow{f}\right\}^{b(m)} = \left[\overleftrightarrow{K}\right]\left\{u^{b(m)}\right\} - \left\{\overleftrightarrow{f}\right\}^{b(m)} \tag{9a}$$

Rewriting Equation 9a for a contact and non-contact boundaries gives:

$$\begin{Bmatrix} \left\{p_0^{b(m)}\right\} \\ \left\{p_i^{b(m)}\right\} \end{Bmatrix} = \begin{bmatrix} \left[\overleftrightarrow{K}_{00}\right]^b & \left[\overleftrightarrow{K}_{0i}\right]^b \\ \left[\overleftrightarrow{K}_{i0}\right]^b & \left[\overleftrightarrow{K}_{ii}\right]^b \end{bmatrix} \begin{Bmatrix} \left\{u_0^{b(m)}\right\} \\ \left\{u_i^{b(m)}\right\} \end{Bmatrix} - \begin{Bmatrix} \left\{\overleftrightarrow{f}\right\}^{b(m)} \\ \left\{\overleftrightarrow{f}\right\}^{b(m)} \end{Bmatrix} \tag{9b}$$

From Equation 9b, the displacement $\left\{u_0^{b(m)}\right\}$ can be obtained as:

$$\left\{u_0^{b(m)}\right\} = \left[\overleftrightarrow{K}_{00}\right]^{b^{-1}} \left(\left\{p_0^{b(m)}\right\} - \left[\overleftrightarrow{K}_{oi}\right]^b \left\{u_i^{b(m)}\right\} + \left\{\overleftrightarrow{f}_0\right\}^{b(m)}\right) \tag{10}$$

and then $\left\{p_i^{b(m)}\right\}$ can be solved for from

$$\left\{p_i^{b(m)}\right\} = [K]_{BB}\left\{u_i^{b(m)}\right\} + \left\{\underline{f}\right\} \tag{11a}$$

where $$[K]_{BB} = \left[\overleftrightarrow{K}_{ii}\right]^b - \left[\overleftrightarrow{K}_{i0}\right]^b \left[\overleftrightarrow{K}_{00}\right]^{b^{-1}} \left[\overleftrightarrow{K}_{0i}\right]^b$$

$$\left\{\underline{f}\right\} = \left[\overleftrightarrow{K}_{i0}\right]^b \left[\overleftrightarrow{K}_{00}\right]^{b^{-1}} \left(\left\{p_o^{b(m)}\right\} + \left\{\overleftrightarrow{f}_0\right\}^{b(m)}\right) - \left\{\overleftrightarrow{f}_i\right\}^{b(m)}$$

Then Equation 11a is multiplied by the $[E]$ matrix

$$[E]\left\{p_i^{b(m)}\right\} = [E][K]_{BB}[E]^T[E]\left\{u_i^{b(m)}\right\} + [E]\left\{\underline{f}\right\} \tag{11b}$$

where the $[E]$ matrix is given by

$$[E] = \begin{bmatrix} [0]_{00} & [0]_{1b} \\ [0]_{b1} & [I]_{bb} \end{bmatrix}$$

Therefore Equation11b can be rewritten as

$$\begin{Bmatrix} \{0\} \\ \left\{p_i^{b(m)}\right\} \end{Bmatrix} = \begin{bmatrix} [0] & [0] \\ [0] & [K]_{BB} \end{bmatrix} \begin{Bmatrix} \{0\} \\ \left\{u_i^{b(m)}\right\} \end{Bmatrix} + \begin{Bmatrix} \{0\} \\ \{\underline{f}\} \end{Bmatrix} \tag{11c}$$

where the subscript *BB* denotes the degree of freedom for the contact part between the boundary element and the finite element domains.

Combining Equation 5, Equation 7 and Equation 11c to give

$$\begin{bmatrix} [K_{00}]^f & [K_{0i}]^f \\ [K_{i0}]^f & [K_{ii}]^f + [K]_{BB} \end{bmatrix} \begin{Bmatrix} \{u_0\}^f \\ \{u_i\} \end{Bmatrix} = \begin{Bmatrix} \{p_1\}^f \\ -\{\underline{f}\} \end{Bmatrix} \tag{12}$$

where Equation 12 is the coupling equation of the boundary element and the finite element. When {*ui*} is solved, it is substituted into Equation 10 to solve for the displacements of the non-contact nodes in the boundary element domain.

From this coupling procedure, it is seen that the finite element package and the boundary element package only need to be slightly adjusted, for example by directly inserting the boundary element into the finite element procedure.

3. FORMULATION OF THE BOUNDING SURFACE MODEL TO ISOTROPIC COHESIVE SOILS

Following Dafalias and Herrmann's papers (1986, 1987), the explicit form of the transformation matrix [*D*] is given by the *Dijkl* tensor determined by using the associated flow rule in the following form:

$$\begin{aligned} D_{ijkl} &= G(\delta_{ki}\delta_{lj} + \delta_{kj}\delta_{li}) + (K - \frac{2}{3}G)\delta_{ij}\delta_{kl} \\ &- \frac{h(L)}{B}\left[3KF_{,\bar{I}}\,\delta_{ij} + \frac{G}{J}F_{,\bar{J}}\,\delta_{ij} + \frac{\sqrt{3}G}{\cos(3\alpha)}\frac{F_{,\alpha}}{bJ}\left(\frac{s_{in}s_{nj}}{J^2} - \frac{3S^3 s_{ij}}{2J^4} - \frac{2\delta_{ij}}{3}\right)\right] \\ &\left[3KF_{,\bar{I}}\,\delta_{kl} + \frac{G}{J}F_{,\bar{J}}\,s_{kl} + \frac{\sqrt{3}G}{\cos(3\alpha)}\frac{F_{,\alpha}}{bJ}\left(\frac{s_{kn}s_{nl}}{J^2} - \frac{3S^3 s_{kl}}{2J^4} - \frac{2\delta_{kl}}{3}\right)\right] \end{aligned} \tag{13}$$

in which

$$L = \frac{1}{B}\left\{3KF_{,\bar{I}}\,\varepsilon_{kk} + \frac{G}{J}F_{,\bar{J}}\,s_{ij}\,\dot{\varepsilon}_{ij} + \frac{\sqrt{3}G}{\cos(3\alpha)}\frac{\dot{F}_{,\alpha}}{bJ}\left[\left(\frac{s_{ik}s_{kj}}{J^2} - \frac{3S^3 s_{ij}}{2J^4}\right)\dot{\varepsilon}_{ij} - \frac{2\dot{\varepsilon}_{kk}}{3}\right]\right\} \tag{13a}$$

$$B = K_p + 9K(F_{,\bar{I}})^2 + G(F_{,\bar{J}})^2 + G(\frac{F_{,\alpha}}{bJ}) \tag{13b}$$

$$K = \frac{1+e_{in}}{3\kappa}(\langle I - I_l\rangle + I_l) \tag{13c}$$

$$K_p = \bar{K}_p + \hat{H}\left\langle\frac{b}{b-1} - s\right\rangle^{-1} \tag{13d}$$

$$\bar{K}_p = \frac{1+e_{in}}{\lambda-\kappa}\left(\left\langle 1 - \frac{I_l}{I_o}\right\rangle + \frac{I_l}{I_o}\right)3F_{,\bar{I}}\,(F_{,\bar{I}}\,\bar{I} + F_{,\bar{J}}) \tag{13e}$$

$$\hat{H} = \frac{1-e_{in}}{\lambda-\kappa}(9F^2_{,\bar{I}} + \frac{1}{3}F^2_{,\bar{J}})P_a\left[z^m h(\alpha) + (1-z^m)h_0\right] \tag{13f}$$

$$z = \frac{3JR\sqrt{3}}{MI_o} \tag{13h}$$

In the bounding surface model, a total of 14 constants are required. The constants κ, λ, G or ν, and $Nc = Mc/(3\sqrt{3})$, $Ne = Me/(3\sqrt{3})$ are the material constants within the critical-state soil mechanics context. The κ and λ can be determined by consolidation and rebound of triaxial specimens, G from the initial slope of deviatoric stress-strain curves, or by assuming a constant Poisson ratio ν and obtaining $G = 3K(1-2\nu)/\{2(1+\nu)\}$. *Nc* and *Ne* are determined by the friction angle at failure in compression and extension. The *Rc, Re, Ac, Ae* and *T* determine the shape of the bounding surface in compression and extension, the first two for ellipse 1, the second two for the hyperbola, and *T* for ellipse 2. The *C, s* and *hc, he* are related to the response for overconsolidated states, the first determining the projection centre *Ic* , the second the size of the elastic nucleus, the last two are the values of the shape hardening factor in compression and extension. All these constants can be determined by carrying out triaxial tests. Usually, *I*l and m can be fixed at values of *Il* = 10 kPa and *m* = 0.02, hence they are not included in the set of model constants.

4. SOIL-STRUCTURE INTERACTION BY USING NONLINEAR SOIL MODEL

The strong earthquake record employed is one of those recorded during the Loma Prieta earthquake of 17th October 1989. The initial twenty seconds containing the main part of the earthquake (maximum acceleration=0.433g) are used as the input motion.
Two structures, a 6-storey and a 12-storey frame [Jury, 1978], will be employed to investigate the structural response. The 6-storey frame has a fundamental period of 0.755 seconds while the 12-storey frame has a fundamental period of 1.88 seconds. Because the purpose is to investigate the effect of the non-linear soil model on structural response, a direct comparison is carried out between the linear and non-linear soil-structure interaction using the values in Table 1 for the constants in the bounding surface model. It is known (Zhang, 1999) that a strong motion earthquake will cause strongly non-linear soil behaviour. Weak motion, however, can be approximated by a linear analysis. In this investigation, a intermediate motion will be used so that the acceleration time history of Loma Prieta earthquake is scaled by a factor of 4. The result is that the predominant period is not changed.
In the following, the scaled Loma Prieta earthquake is directly employed to investigate 6 and 12 storey frames when the soil is represented by linear and non-linear soil models. The non linear soil parameters required were given in the previous section while the assumed linear properties required are only G and .

Table 1 Constants in bounding surface model

λ	κ	N_c	N_e	R_c	R_e	A_c	A_e
0.29	0.04	0.26	0.21	2.0	0.0	0.4	0.0

T	C	S	H_C	H_e	ν	void ratio
0.01	0.3	0.0	6.0	6.0	0.3	1.04

4.1 6-Storey Frame

Usually when a linear soil model is employed, there is no permanent settlement of the foundation after the earthquake analyses. This contradicts the results from many earthquake investigations. A non-linear soil model can illustrate this problem. Because the soil has strong non-linear properties, deformation will occur when loading the soil. Although unloading results in resilience, permanent deformation still remains so that settlement of the foundation occurs. Figure 1 shows the time history for the permanent settlement of the foundation caused by the scaled earthquake.

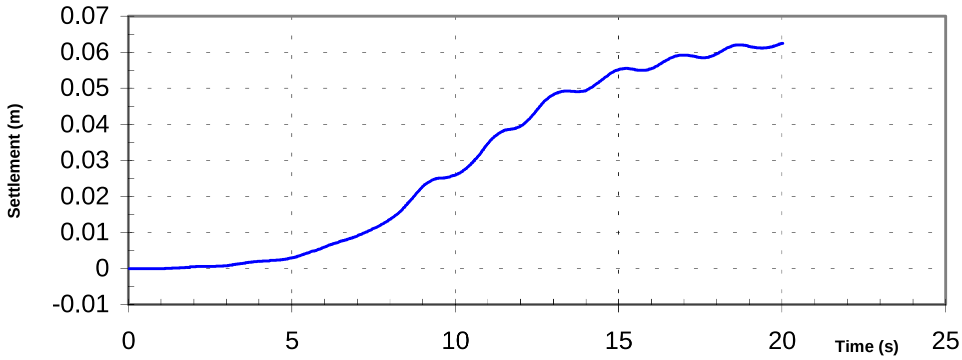

Figure 1 Settlement of Foundation of 6-Storey Frame

The accelerations and displacements at the top floor are shown in Figure 2 for the linear and non-linear soil models. From the figures, it is easy to see that the maximum acceleration on the top floor for the linear soil model is greater than that for the non-linear soil model and the acceleration time histories are similar but different. The maximum displacement at the top floor for the linear soil model is greater than that for the non-linear model. There are two reasons for this result. One is that the permanent settlement of the foundation reduces structural vibration. The other is that elastic-plastic soil extends the system period of the soil and structure so that it is shifted away from the predominant excitation period of the earthquake.

4.2 12-Storey Frame

For the 12-storey frame, the settlement time history of the foundation is shown in Figure 3. When compared with Figure 1, the permanent settlement of the foundation of the 12 storey frame is greater but they show similar

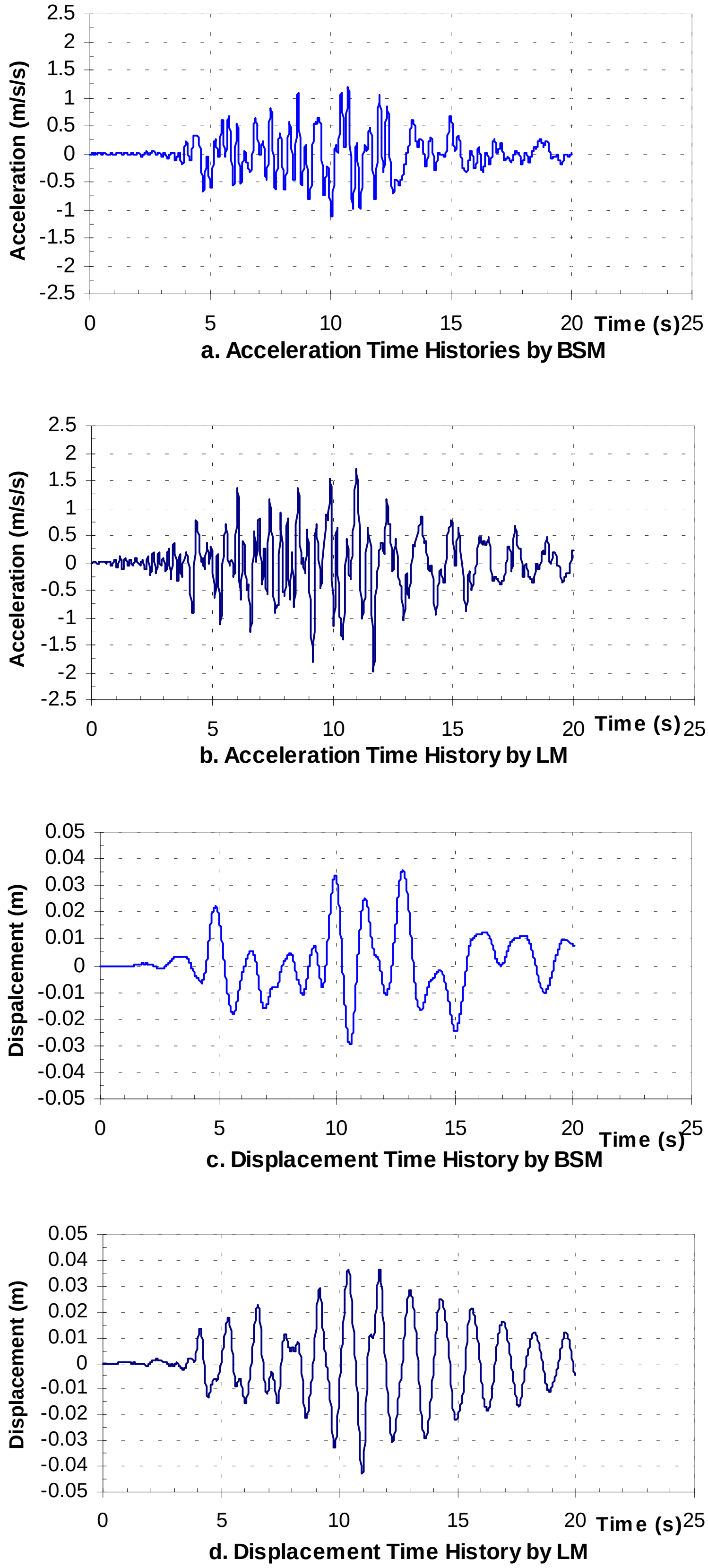

Figure 2 Comparisons of Acceleration and Displacement Time Histories at the Top Floor for 6-Storey Frame
BSM: Bounding Surface Model LM: Linear Model

characteristics. Since the 12 storey building has about twice the gravity loading of the 6 storey building, the non linear analysis shows that the settlements are not in direct proportions.

When the non-linear soil model is employed, the acceleration time history and the displacement time history at the top floor are shown in Figure 4. In a similar manner to the 6-storey frame, the maximum acceleration and displacement in the linear analysis are greater than those in the non-linear analysis. However, when compared with the results of the 6-storey frame, the difference in the acceleration at the top floor between the linear and non-linear analyses is greater.

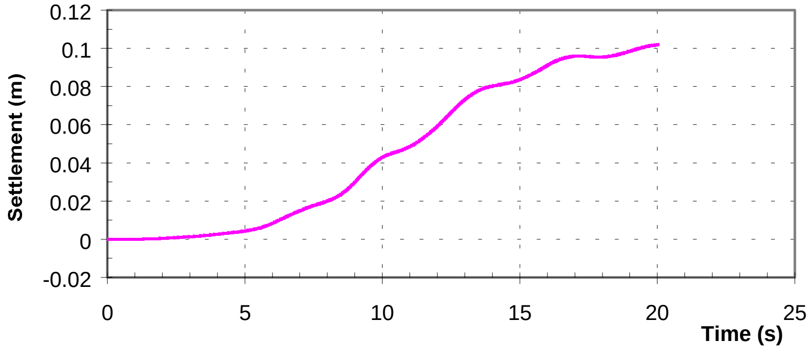

Figure 3 Settlement of Foundation of 12 Storey-Frame

5. SUMMARY

When the near field is considered as an elasto-plastic material and far field is considered to be a linear material, the direct coupled method of boundary element and finite element can be used in the analysis. For the Loma Prieta earthquake, the investigation shows the structural response in the non-linear analysis is less than that in the linear analysis regardless of the acceleration or displacement at the top floor.

6. REFERENCES

Dafalias Y.F, Herrmann L.R, (1986) "Bounding Surface Plasticity: Application to Isotropic Cohesive Soils", *Journal of Engineering Mechanics*, Vol.112, pp. 1263-1291

Herrmann L. R, Kaliakin V, Shen C. K, Mish K. D, Zhu Z.Y, (1987) "Numerical Implementation of Plasticity Model for Cohesive Soils", *Journal of Engineering Mechanics*, No.4, Vol.113, pp. 500-519.

Jury, R.D., (1978) "Seismic Load Demands on Columns of Reinforced Concrete Multi-storey Frames", Research *Report No. 78-12*, Department of Civil Engineering, University of Canterbury, Christchurch, New Zealand.

Zhang J.J., (1999) "*Seismic Soil-Structure Interaction in Time Domain*", Thesis for the Degree of Doctor of Philosophy in Civil Engineering at the University of Canterbury, (to be submitted).

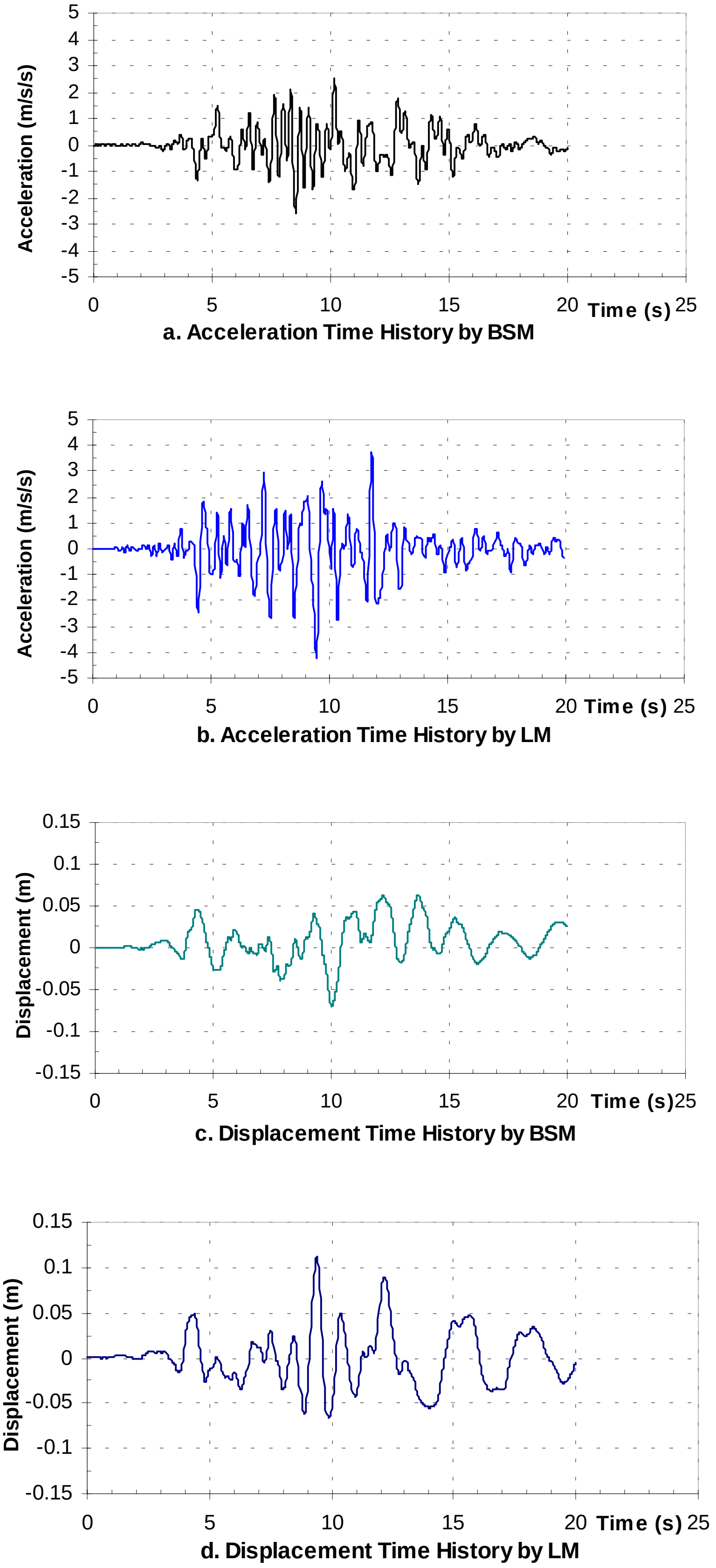

Figure 4 Comparisons of Acceleration and Displacement Time Histories at the Top Floor for 12-Story Frame BSM: Bounding Surface Model LM: Linear Model